Robust analysis of design in vibration of turbomachines

M. Mbaye, Christian Soize, J.-P. Ousty, Evangéline Capiez-Lernout

ROBUST ANALYSIS OF DESIGN IN VIBRATION OF TURBOMACHINES

Moustapha Mbaye [1,2] , **Christian Soize**[1] *, **Jean-Philippe Ousty**[2] , **Evangeline Capiez-Lernout**[1]
[1] Université Paris-Est, Laboratoire de Modélisation et Simulation Multi Echelle
MSME UMR 8208 CNRS, 5 bd Descartes, 77454 Marne-la-Vallée, France
[2] Turbomeca - Safran Group, 64511 Bordes, France
moustapha.mbaye@univ-paris-est.fr, christian.soize@univ-paris-est.fr
jean-philippe.ousty@turbomeca.fr, evangeline.capiezlernout@univ-paris-est.fr

In the context of turbomachinery design, a small variation in the blade characteristics due to manufacturing tolerances can affect the structural symmetry creating mistuning which increases the forced response. However, it is possible to detune the mistuned system in order to reduce the forced response amplification. The main technological methods to introduce detuning are based on modifying either the blade material properties, either the interface between blades and disk, or the blade shapes. This paper presents a robustness analysis of mistuning for a given detuning in blade geometry. Detuning is performed by modifying blade shapes. The different types of blades, obtained by those modifications, are then distributed on the disk circumference. A new reduced-order model of the detuned disk is introduced. It is based on the use of the cyclic modes of the different sectors which can be obtained from a usual cyclic symmetry modal analysis. Finally, the robustness of the computational model responses with respect to uncertainties, is performed with a stochastic analysis using a nonparametric probabilistic approach of uncertainties which allows both the system-parameter uncertainties and the modeling errors to be taken into account.

1 INTRODUCTION

Small variations in the blade characteristics of cyclic structures due to manufacturing tolerances affect the structural cyclic symmetry creating mistuning which increases the forced response amplitudes (e.g. see [1–3]). However, it is possible (e.g. see [4–8]) to intentionally detune the mistuned system in order to reduce the forced response amplification. The main technologic solutions to introduce detuning are based on modifying blade material properties, the interface between blade and disk, or the blade shape by introducing several types of blades with different geometries corresponding to geometrical modifications of the nominal blades. In the present paper, it is assumed that detuning is performed by modifying blade shapes and the disk is not mistuned.

Vibration analysis of cyclic structures is usually performed using their cyclic symmetry and formulated for one sector from which the dynamics of the structure is obtained. This is no longer the case for mistuned and/or detuned structures which need a full structure formulation. To reduce numerical computational costs while solving the mistuning problem on finite element meshes of realistic bladed disks, many reduced-order methods have been introduced (see [6, 9–16]). In general, reduced-order models are obtained by substructuring a bladed disk into disk and blades components (see e.g. [9, 10]), as this allows an easy implementation of blade mistuning. However, a different approach [11] called SNM has been proposed by Yang and Griffin, in which the tuned system cyclic modes are used without substructuring to generate a reduced-order model. This technique is very efficient in the case of cyclic structures with blade material properties modifications but may be inefficient for the case of blade geometric modifications for the following reasons. It is well known that the tuned modes constitute a basis of the admissible space of the displacements for the mistuned bladed disk. Nevertheless, such a basis is generally not really efficient with respect to the convergence speed and a large number of tuned modes are required for such a case. It should be noted that, if convergence is slow, then the reduced-order model is not sufficiently small and so would not be efficient and effective to implement the probabilistic model of uncertainties and above all, to perform a robust design optimization. In another hand, it is well recognized today that, if the use of the tuned modes for constructing the reduced-order model is efficient for blade material properties modifications, it is not always the case for blade geometric modifications (see for instance [14, 17]). In addition, the blade geometric modifications induce a problem related to incompatibility representations between the tuned modes calculated with the mesh of the tuned bladed disk and the structural matrices of the geometrically modified bladed disk calculated with another mesh. In these conditions, the nominal and the geometrically modified meshes are incompatible. Consequently, these incompatible finite

*Adress all correspondance to this author.

element meshes induce a difficulty for constructing the projection of the geometrically modified mass and stiffness matrices using the tuned bladed disk sector cyclic modes. That is why, in [11], proportional mistuning by perturbing the Young moduli of individual blades is only simulated. A simple model derived from SNM and known as the Fundamental Mistuning Model (FMM) that reduces the set of nominal modes to a single modal family [12, 13], had also been introduced. Nevertheless, its application field is limited to a modal family with nearly equal frequency. An extension of the FMM, for the case in which all modes of the family do not share the same frequency, known as Asymptotic Mistuning model (AMM), has also been introduced in [15, 16]. This method is a perturbation method in which the small parameters are the small frequency corrections induced by mistuning and the small damping of the tuned modes, or the first aerodynamic correction of the purely structural vibration characteristics. Consequently, large geometric detuning can be difficult to take into account with such a method. To solve the problem of geometric detuning, without using substructuring, a method named Static Mode Compensation (SMC) has been proposed in [14], and used in [18], in which the mistuned system is represented by the full tuned system and by virtual mistuning components. But this method needs a convergence acceleration to be performed, which requires a large amount of computation. It should also be noted that a new method has been proposed by Sinha in [17] in order to improve the SNM method. It consists in including tuned modes with blades having geometries perturbed along important proper orthogonal decomposition (POD) features as basis functions.

In this paper, for solving the problem of detuning with geometric modification, it is assumed that a commercial software (black box) is used to compute the cyclic modes and mass and stiffness matrices of the different bladed disk sector types in independent calculations. In this particular context, we propose here a new method which uses the cyclic modes of the different bladed disk sectors and which consist on reducing each sector mass and stiffness matrices by its own modes. Linear constraints are then applied on common boundaries between sectors to make the displacement field admissible. The purpose of this paper for the proposed reduced-order model is to build a reduced-order model which can solve large geometric mistuning for an optimization over the detuning pattern of the different blade geometries. This reduction method is different to the one proposed in [17] by the way it uses the real modes of each sector instead of using tuned modes of blades having geometries perturbed along important POD. This reduction method has already been developed in [19]. An application is done on a realistic bladed disk model by comparing its forced responses using this reduction method and a full model.

The random nature of blade mistuning due to manufacturing tolerances and dispersion of materials has been a motivation to construct a stochastic model of uncertainties in order to perform a statistical analysis for a robust prediction of the effects of mistuning. In this context we use the nonparametric probabilistic approach of uncertainties which allows a prior stochastic model to be constructed in taking into account both the system-parameter uncertainties and the model uncertainties induced by modeling errors. This nonparametric probability model is directly constructed using the mean reduced matrix model, and the Maximum entropy (MaxEnt) principle under the constraints defined by the available information.

2 CONSTRUCTION OF THE MEAN REDUCED MODEL

The reduced model is built using the reduced-order method presented in [19] which is an extension of the approach proposed by Yang and Griffin in [11], and which takes into account geometrical modifications of blades. Instead of projecting perturbed mass and stiffness matrices on a basis of tuned cyclic modes, the method proposed consists in projecting the mass and stiffness matrices of a sector on a basis of its own cyclic modes, and in assembling the whole bladed disk reduced model by insuring the displacement-field continuity between all the adjacent sectors.

2.1 Dynamic equation of the detuned system

Let us consider the finite element model of a detuned structure with N blades, with detuning resulting from geometrical modifications of some blades. The frequency band is $\mathcal{B} = [\omega_{min}, \omega_{max}]$ with $0 < \omega_{min} < \omega_{max}$. For the frequency band B, the mean (or nominal) computational model of the detuned bladed disk is written as

$$(-\omega^2[\underline{M}] + j\omega[\underline{D}] + [\underline{K}])\underline{\mathbf{u}}(\omega) = \underline{\mathbf{f}}_{exc}(\omega) + \underline{\mathbf{f}}_{aero}(\omega, \underline{\mathbf{u}}(\omega)), \tag{1}$$

with $j^2 = -1$ and where $\underline{\mathbf{f}}_{exc}$ is the vector of unsteady forces applied to the blades and due to an aerodynamic excitation source. In the above equation, $\underline{\mathbf{f}}_{aero}$ represents the vector of unsteady aeroelastic forces applied to the blades due to the blades deformations. The vector, $\underline{\mathbf{u}}$, is the finite element discretization of the displacement field of the complete detuned structure. Finally, the matrices $[\underline{M}]$, $[\underline{D}]$ and $[\underline{K}]$ are the mass, damping and stiffness matrices. The dimension of vector $\underline{\mathbf{u}}$ is n_{dof} which represents the number of degrees-of-freedom of the computational model. Linear constraints relationships must be added to Eq.(1). The constraints are written between what we call the vector of constrained degrees-of-freedom $\underline{\mathbf{u}}_c(\omega)$ and the vector of free degrees-of-freedom $\underline{\mathbf{u}}_\ell(\omega)$. The vector $\underline{\mathbf{u}}(\omega)$ can then be written

$$\underline{\mathbf{u}}(\omega) = (\underline{\mathbf{u}}_\ell(\omega), \underline{\mathbf{u}}_c(\omega)), \tag{2}$$

where

$$\underline{\mathbf{u}}_c(\omega) = [\underline{B}]\,\underline{\mathbf{u}}_\ell(\omega). \tag{3}$$

For the entire detuned bladed disk, the constraint equation is then written as

$$\underline{\mathbf{u}}(\omega) = [\underline{\mathbb{B}}]\,\underline{\mathbf{u}}_\ell(\omega). \tag{4}$$

Introducing the dynamic stiffness matrix

$$[\underline{E}(\omega)] = -\omega^2[\underline{M}] + j\omega[\underline{D}] + [\underline{K}], \tag{5}$$

the dynamic equation Eq. (1), which integrates the constraints relationships, becomes

$$[\underline{\mathbb{B}}]^T[\underline{E}(\omega)][\underline{\mathbb{B}}]\,\underline{\mathbf{u}}_\ell(\omega) = [\underline{\mathbb{B}}]^T(\underline{\mathbf{f}}_{exc}(\omega) + \underline{\mathbf{f}}_{aero}(\omega, [\underline{\mathbb{B}}]\underline{\mathbf{u}}_\ell(\omega)). \tag{6}$$

The detuned bladed disk is made of N sectors compatible on their coupling interfaces. Consequently, the dynamic stiffness matrix is made up of $N \times N$ sub-matrices, each one having $\overline{n} \times \overline{n}$ components. The displacements and forces vectors are constituted of N sub-vectors. We then have,

$$[\underline{E}] = \begin{pmatrix} [\underline{E}]^0 & \cdots & [0] \\ \vdots & \ddots & \vdots \\ [0] & \cdots & [\underline{E}]^{N-1} \end{pmatrix}, \tag{7}$$

$$\underline{\mathbf{u}} = \begin{pmatrix} \underline{\mathbf{u}}^0 \\ \vdots \\ \underline{\mathbf{u}}^{N-1} \end{pmatrix}, \quad \underline{\mathbf{f}} = \begin{pmatrix} \underline{\mathbf{f}}^0 \\ \vdots \\ \underline{\mathbf{f}}^{N-1} \end{pmatrix}, \tag{8}$$

for which the vector $\underline{\mathbf{u}}^p$ contains the displacements of the $\overline{n}$ degrees-of-freedom associated with sector p. For a given sector, this number involves its inner and boundaries degrees-of-freedom. The boundaries degrees-of-freedom are common to the two adjacent sectors. It should be noted that matrix $[\underline{E}]$ is a bloc diagonal matrix. Therefore, the mass and stiffness matrices are written as

$$[\underline{M}] = \begin{pmatrix} [\underline{M}]^0 & \cdots & [0] \\ \vdots & \ddots & \vdots \\ [0] & \cdots & [\underline{M}]^{N-1} \end{pmatrix}, \tag{9}$$

$$[\underline{K}] = \begin{pmatrix} [\underline{K}]^0 & \cdots & [0] \\ \vdots & \ddots & \vdots \\ [0] & \cdots & [\underline{K}]^{N-1} \end{pmatrix}, \tag{10}$$

where the $\overline{n} \times \overline{n}$ sector mass and stiffness matrices, $[\underline{M}]$ and $[\underline{K}]$, are symmetric matrices. We have

$$[\underline{M}]^p = \begin{pmatrix} [\underline{M}_{\ell\ell}] & [\underline{M}_{\ell i}] & [0] \\ [\underline{M}_{\ell i}]^T & [\underline{M}_{ii}] & [\underline{M}_{ir}] \\ [0] & [\underline{M}_{ir}]^T & [\underline{M}_{rr}] \end{pmatrix}, \tag{11}$$

$$[\underline{K}]^p = \begin{pmatrix} [\underline{K}_{\ell\ell}] & [\underline{K}_{\ell i}] & [0] \\ [\underline{K}_{\ell i}]^T & [\underline{K}_{ii}] & [\underline{K}_{ir}] \\ [0] & [\underline{K}_{ir}]^T & [\underline{K}_{rr}] \end{pmatrix}, \tag{12}$$

where subscripts i, ℓ and r are related to the inner, the left side coupling interface and the right side coupling interface degrees-of-freedom. At this step, the dynamic system operators and displacement vector are expressed in local blade coordinates system associated with each sector Ω_p, for all p in $\{0, 1, \ldots, N-1\}$.

2.2 Reduced order model

The reduced-order model is constructed by using a modal basis $[\underline{\Psi}]^{proj}$ of real modes obtained in the global cyclic coordinates system. This projection basis $[\underline{\Psi}]^{proj}$ is obtained by using an initial basis $[\underline{\Psi}]$ of non continuous modes which are put in phase. For more details about the projection basis, we refer the reader to [19].

2.2.1 Generalized dynamic equation of the detuned system

The displacement vector is written as

$$\underline{\mathbf{u}}(\omega) = [\underline{\Psi}^{proj}]\underline{\mathbf{q}}(\omega), \tag{13}$$

where the complex vector $\underline{\mathbf{q}} = (\underline{\mathbf{q}}_0, \ldots, \underline{\mathbf{q}}_{N-1})$ is made up of all the generalized coordinates associated with the system. In the global coordinates system, the reduced-order computational model is thus written as

$$\begin{aligned}[\underline{E}_{red}(\omega)]\underline{\mathbf{q}}(\omega) =& [\underline{\Psi}^{proj}]^T\underline{\mathbf{f}}_{exc}(\omega) + \\ & [\underline{\Psi}^{proj}]^T\underline{\mathbf{f}}_{aero}(\omega, [\underline{\Psi}^{proj}]\underline{\mathbf{q}}(\omega)),\end{aligned} \tag{14}$$

Using Eq.(7) and the expression of matrix $[\underline{\Psi}^{proj}]$, it can be deduced that the reduced dynamic stiffness matrix, $[\underline{E}_{red}(\omega)]$, is fully populated and we have,

$$[\underline{E}_{red}(\omega)] = [\underline{\Psi}^{proj}]^T[\underline{E}(\omega)][\underline{\Psi}^{proj}], \tag{15}$$

$$[\underline{E}_{red}(\omega)]_{\beta,\alpha} = \sum_{p=0}^{N-1} \left((\underline{\Psi}^{proj})_\beta^{\Omega_p}\right)^T [\underline{E}(\omega)]^{pp} \left((\underline{\Psi}^{proj})_\alpha^{\Omega_p}\right). \tag{16}$$

The generalized forces are defined by

$$\begin{aligned}&\underline{\mathbf{g}}_{exc}(\omega) = [\underline{\Psi}^{proj}]^T\underline{\mathbf{f}}_{exc}(\omega), \\ &\underline{\mathbf{g}}_{aero}(\omega, \underline{\mathbf{q}}(\omega)) = [\underline{\Psi}^{proj}]^T\underline{\mathbf{f}}_{aero}(\omega, [\underline{\Psi}^{proj}]\underline{\mathbf{q}}(\omega)).\end{aligned} \tag{17}$$

Clearly, the projection basis is constructed with respect to the distribution of the different sector types and by keeping orthogonality properties between modes. Note that the reduced

dynamic stiffness operator exhibits off diagonal terms. This implies that the detuning couples tuned cyclic modes with different number of nodal diameters. The aerodynamic generalized forces can be expressed by introducing an aeroelastic matrix such that

$$\underline{\mathbf{g}}_{aero}(\omega,[\underline{\Psi}^{proj}]\,\underline{\mathbf{q}}(\omega)) = -[\underline{A}_{red}(\omega)]\,\underline{\mathbf{q}}(\omega). \tag{18}$$

The real part and the imaginary parts of this aeroelastic matrix depend on ω and the imaginary part can be viewed as a "damping" matrix. We then write this aeroelastic matrix as

$$[\underline{A}_{red}(\omega)] = [\underline{A}^R_{red}(\omega)] + j\,[\underline{A}^I_{red}(\omega)]. \tag{19}$$

The reduced-order computational model can then be rewritten as

$$\begin{aligned}\{-\omega^2[\underline{M}_{red}]+j\omega([\underline{D}_{red}]+[\underline{A}^I_{red}(\omega)])+[\underline{K}_{red}]+ \\ [\underline{A}^R_{red}(\omega)]\}\underline{\mathbf{q}}(\omega) = \underline{\mathbf{g}}_{exc}(\omega),\end{aligned} \tag{20}$$

2.2.2 Particular case of a structural damping introduced by a modal damping ratio

The way the reduced structural damping matrix is written by using the projection basis $[\underline{\Psi}^{proj}]$ depends on the way structural damping is taken into account. In fact, when damping is taken into account by a fully populated matrix or a matrix expressed in function of the mass and the stiffness matrices ($[\underline{D}] = a[\underline{M}] + b[\underline{K}]$), the reduced structural damping matrix is fully populated with this projection basis. Although, if a modal damping ratio is considered, it is necessary to diagonalize the structural mass and stiffness reduced matrices to be able to write the reduced structural damping matrix in a diagonal form. To do so, the generalized eigenvalue problem associated with the conservative structural reduced-order computational model (without damping forces nor aerodynamic forces) is solved at first,

$$([\underline{K}_{red}] - \lambda[\underline{M}_{red}])\underline{\mathbf{y}} = 0, \tag{21}$$

where λ is an eigenvalue and $\underline{\mathbf{y}}$ is the associated eigenvector. Since matrices $[\underline{K}_{red}]$ and $[\underline{M}_{red}]$ are real and symmetric, the eigenvectors are real and verify the orthogonality property,

$$< [\underline{K}_{red}]\,\underline{\mathbf{y}}^{\alpha}, \underline{\mathbf{y}}^{\beta} >= \omega_{\alpha}^2\,\mu_{\alpha}\,\delta_{\alpha\beta}, \tag{22}$$

$$< [\underline{M}_{red}]\,\underline{\mathbf{y}}^{\alpha}, \underline{\mathbf{y}}^{\beta} >= \mu_{\alpha}\delta_{\alpha\beta}, \tag{23}$$

where μ_{α} and ω_{α} are the generalized mass and the eigenfrequency for the mode α. By choice, the reduced structural damping matrix is written as a diagonal matrix

$$< [\underline{D}_{red}]\,\underline{\mathbf{y}}^{\alpha}, \underline{\mathbf{y}}^{\beta} >= 2\,\xi_{\alpha}\,\omega_{\alpha}\,\mu_{\alpha}\,\delta_{\alpha\beta}, \tag{24}$$

where ξ_{α} is the modal damping ratio associated with mode α. Note that, in the global coordinates system, the real modes $\underline{\mathbf{u}}^{\alpha}$ of the detuned bladed disk are written as

$$\underline{\mathbf{u}}^{\alpha} = [\underline{\Psi}^{proj}]\,\underline{\mathbf{y}}^{\alpha}. \tag{25}$$

Let $[\underline{y}]$ be the matrix whose columns are the vectors $\underline{\mathbf{y}}^{\alpha}$. Let us introduce a new variable $\underline{\eta}$ such that $\underline{q}(\omega) = [\underline{y}]\underline{\eta}(\omega)$. Then the generalized problem becomes

$$\{-\omega^2[\underline{M}_{diag}] + j\omega[\underline{D}_{diag}] + [\underline{K}_{diag}]\}\underline{\eta}(\omega) = [\underline{y}]^T\underline{\mathbf{g}}_{exc}(\omega), \tag{26}$$

where $[\underline{M}_{diag}]$, $[\underline{K}_{diag}]$ and $[\underline{D}_{diag}]$ are diagonal and are written as

$$[\underline{M}_{diag}] = [\underline{y}]^T[\underline{M}_{red}][\underline{y}] = \begin{pmatrix} \mu_1 & \cdots & 0 \\ \vdots & \ddots & \vdots \\ 0 & \cdots & \mu_m \end{pmatrix}, \tag{27}$$

$$[\underline{K}_{diag}] = [\underline{y}]^T[\underline{K}_{red}][\underline{y}] = \begin{pmatrix} \omega_1^2\mu_1 & \cdots & 0 \\ \vdots & \ddots & \vdots \\ 0 & \cdots & \omega_m^2\mu_m \end{pmatrix}, \tag{28}$$

$$[\underline{D}_{diag}] = [\underline{y}]^T[\underline{D}_{red}][\underline{y}] = \begin{pmatrix} 2\xi_1\omega_1\mu_1 & \cdots & 0 \\ \vdots & \ddots & \vdots \\ 0 & \cdots & 2\xi_m\omega_m\mu_m \end{pmatrix}. \tag{29}$$

3 VALIDATION OF THE REDUCTION METHOD

A validation of this reduction method has already been provided in [19]. In this part, another test case configuration is only presented. The test case considered here is an industrial blisk with 23 blades. The commercial software, ANSYS, is used to compute the cyclic modes and the mass and stiffness matrices for constructing the reduced-order model inputs, and the forced response of the 360-deg full-rotor model. For the detuned system, four other types of blades are created from the nominal one by shape modifications of the blade upper part (see Fig. 1). Then a detuned bladed disk with 5 different blades is obtained. The bladed disk is

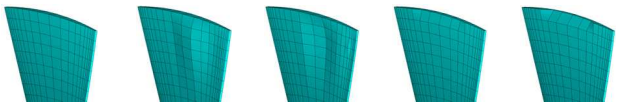

Fig. 1. Finite element models of blades: a reference blade (a) and geometrically modified blades (b-e).

detuned by modifying arbitrarily four of its blades to make them have the shapes shown in Fig. 1. The test case we are going to study is shown in Fig. 2. The forced responses

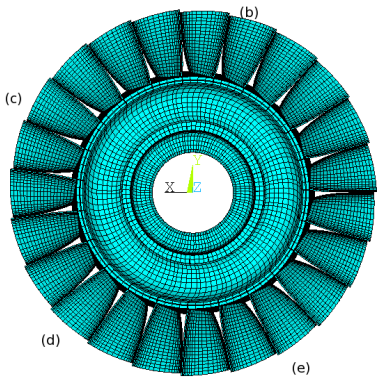

Fig. 2. Complete intentionally detuned bladed disk with arbitrary geometric modifications of four blades.

are displayed in Fig. 3 for an engine order excitation which is 9, for a low level of damping (0.1%) in order to increase the coupling effects and for the frequency band $[4150\,,4550]$ Hz in order to get a comparison between the full and the reduced-order models. The results show a sufficient accu-

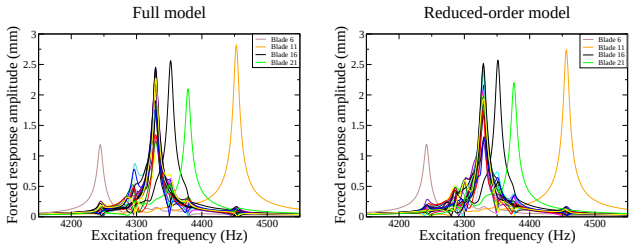

Fig. 3. Forced responses of the 23 blades to an engine order excitation which is 9 and for the frequency band $[4150\,,4550]$ Hz: Full model (left) and reduced-order model (right).

racy of the proposed reduced-order model in capturing the detuned blisk forced responses.

4 NONPARAMETRIC MODEL OF RANDOM UNCERTAINTIES FOR BLADE MISTUNING

The purpose here is to model uncertainties due to mistuning. Mistuning are mainly due to manufacturing tolerances and the framework of the probability theory is well adapted to take into account mistuning. Consequently, a prior stochastic model of uncertainties has to be constructed in order to increase the robustness of the predictions of the computational model with respect to uncertainties. If no experimental data are available, then the prior stochastic model cannot be improved in constructing a posterior stochastic model using the prior stochastic model, the experimental data and the Bayes method. In such a case, the best way to construct the prior stochastic model, is to use Information Theory which is a powerful and validated theory. The Maximum Entropy (MaxEnt)principle of Information Theory allows the prior probability distributions to be constructed under the constraints defined by the available information. It is proven that, if there is no available information related to statistical dependencies between random variables, then the best prior stochastic model given by the MaxEnt is to consider these random variables as independent. In this condition, for the stochastic model of blade uncertainties due to mistuning, it is then assumed a statistical independence from blade to blade, each blade being detuned (intentional mistuning) or not. To take into account both the system-parameter uncertainties and the model uncertainties induced by modeling errors, the nonparametric stochastic model of uncertainties is used. The main results concerning this nonparametric stochastic model to construct a prior stochastic model of uncertainties in structural dynamics can be found in [20, 21]. Such a probabilistic approach requires the construction of a mean reduced matrix model for each uncertain sector. It should be noted that the nominal computational model, that is to say the computational model with the nominal values of the system parameters, presently called the mean computational model, is assumed to be a good computational model. If no experimental data are available to update the nominal values of the parameters, these nominal values are considered as good. If the parametric probabilistic approach was used to take into account system-parameter uncertainties, the prior stochastic model of the uncertain system parameters would be constructed by writing that the mean value of the random system parameters are equal to the nominal values. There is no other solution if no experimental data are available and in the context of Information Theory. When the nonparametric probabilistic approach is used to take into account both the system-parameter uncertainties and model uncertainties induced by modeling errors, the same strategy is used to construct the prior stochastic model of uncertainties. It is thus written that the mean values of the random operators of the computational model are equal to the nominal values of these operators. The introduction of the reduced-order model leads us to introduce C1 below as an available information. In addition, the stochastic model has to be consistent with the mathematical and mechanical properties leading us to introduce C2 and C3 below as an available information. Thus, it has to satisfy the following constraints which constitute the only available information:

- C1: the mean reduced matrix is equal to the mean value of the random reduced matrix;

- C2: the signature of the random reduced matrix is respected: it means that the random reduced matrix has to be positive definite if its corresponding mean reduced matrix is positive definite;

- C3: the second-order moment of the physical random response of the bladed disk has to exist, for getting a second-order displacement field.

The stochastic model of uncertainties is then derived by

using the MAxEnt principle under the constraints defined by constraints C1, C2 and C3.

4.1 Random Reduced Matrix Model for the Bladed-Disk

Using the methodology derived from [3, 20], the nonparametric probabilistic approach consists in modeling the reduced dynamic stiffness matrix for sector p as the random matrix

$$[\mathbf{E}_{red}(\omega)^p] = -\omega^2[\mathbf{M}^p_{red}] + j\omega[\mathbf{D}^p_{red}] + [\mathbf{K}^p_{red}], \qquad (30)$$

in which $[\mathbf{M}^p_{red}]$, $[\mathbf{D}^p_{red}]$ and $[\mathbf{K}^p_{red}]$ are independent random matrices corresponding to the random reduced mass, damping, and stiffness matrices of sector p, and modeling the complex aeroelastic matrix as the random matrix $[\mathbf{A}_{red}(\omega)^p]$. Then, constraint C1 is written as

$$\begin{aligned} \mathcal{E}\left\{[\mathbf{M}^p_{red}]\right\} = [\underline{M}^p_{red}], \quad \mathcal{E}\left\{[\mathbf{D}^p_{red}]\right\} = [\underline{D}^p_{red}], \\ \mathcal{E}\left\{[\mathbf{K}^p_{red}]\right\} = [\underline{K}^p_{red}], \quad \mathcal{E}\left\{[\mathbf{A}^p_{red}]\right\} = [\underline{A}^p_{red}], \end{aligned} \qquad (31)$$

where $\mathcal{E}\{.\}$ is the mathematical expectation. The first step of the implementation of the nonparametric probabilistic approach of uncertainties consists in normalizing the mass, the damping, the stiffness and the aeroelastic random matrices such that the mean value of each normalized random matrix is the unity matrix. Such a construction requires the factorization of the mean reduced matrices. The mean reduced mass, damping and stiffness matrices are real positive definite matrices. So, their Choleski factorization yields

$$\begin{aligned} [\underline{M}^p_{red}] = [\underline{L}^p_M]^T[\underline{L}^p_M], \quad [\underline{D}^p_{red}] = [\underline{L}^p_D]^T[\underline{L}^p_D], \\ [\underline{K}^p_{red}] = [\underline{L}^p_K]^T[\underline{L}^p_K]. \end{aligned} \qquad (32)$$

Then, the real random matrices can be written as

$$\begin{aligned} [\mathbf{M}^p_{red}] = [\underline{L}^p_M]^T[\mathbf{G}^p_M][\underline{L}^p_M], \quad [\mathbf{D}^p_{red}] = [\underline{L}^p_D]^T[\mathbf{G}^p_D][\underline{L}^p_D], \\ [\mathbf{K}^p_{red}] = [\underline{L}^p_K]^T[\mathbf{G}^p_K][\underline{L}^p_K], \end{aligned} \qquad (33)$$

where $[\mathbf{G}^p_M]$, $[\mathbf{G}^p_D]$ and $[\mathbf{G}^p_K]$ are real normalized random matrices whose mean value is the unity matrix. For the complex aeroelastic matrix, we follow the methodology proposed in [21]. A singular value decomposition is used to perform the factorization. By this way, the complex matrix $[\underline{A}_{red}]$ is written as

$$[\underline{A}_{red}(\omega)] = [\underline{U}(\omega)][\underline{T}(\omega)], \qquad (34)$$

in which $[\underline{U}(\omega)]$ is a complex unitary matrix and $[\underline{T}(\omega)]$ is a Hermitian positive definite matrix admitting a Choleski factorization. The stochastic model of the aeroelastic matrix is then written as

$$[\mathbf{A}_{red}(\omega)] = [\underline{U}(\omega)][\underline{L}_T(\omega)]^T[\mathbf{G}_A][\underline{L}_T(\omega)], \qquad (35)$$

where $[\mathbf{G}_A]$ is a real normalized random matrix whose mean value is the unity matrix. Constraints C2 and C3 mean that the normalized random matrices $[\mathbf{G}^p_M]$, $[\mathbf{G}^p_D]$, $[\mathbf{G}^p_K]$ and $[\mathbf{G}_A]$ are real positive definite matrices verifying

$$\begin{aligned} &\mathcal{E}\left\{\|[\mathbf{G}^p_M]^{-1}\|^2_F\right\} < +\infty, \quad \mathcal{E}\left\{\|[\mathbf{G}^p_D]^{-1}\|^2_F\right\} < +\infty, \\ &\mathcal{E}\left\{\|[\mathbf{G}^p_K]^{-1}\|^2_F\right\} < +\infty, \quad \mathcal{E}\left\{\|[\mathbf{G}_A]^{-1}\|^2_F\right\} < +\infty, \end{aligned} \qquad (36)$$

where $\|[.]\|_F = (\mathrm{tr}([.][.]^T))^{\frac{1}{2}}$. The dispersion level of these four normalized random matrices is controlled by the following positive real parameters δ^p_M, δ^p_D, δ^p_K and δ_A which are defined by

$$\delta_F = \left\{ \frac{\mathcal{E}\left\{\|[\mathbf{G}_F] - [\underline{G}_F]\|^2_F\right\}}{[\underline{G}_F]} \right\}^{\frac{1}{2}} \quad \text{with} \quad F = \{\mathbf{M}, \mathbf{D}, \mathbf{K}, \mathbf{A}\}. \qquad (37)$$

From Eqs. (33) and (35), it can be deduced that these parameters allow the dispersion level of random matrices $[\mathbf{M}^p_{red}]$, $[\mathbf{D}^p_{red}]$, $[\mathbf{K}^p_{red}]$ and $[\mathbf{A}_{red}]$ to be controlled.

4.2 Probability Distributions of the Random Matrices

Using the MaxEnt principle with available information defined by constraints C1, C2 and C3 related to normalized random matrices, an explicit algebraic representation of matrix $[\mathbf{G}]$ is introduced and completely defines its probability distribution. Such a representation yields a generator of independent realizations which is used for the Monte Carlo numerical simulation in order to solve the stochastic equation. According to [20] (in which all the details concerning the construction of the stochastic model of the normalized random matrix $[\mathbf{G}]$ can be found), the random matrix $[\mathbf{G}]$ can be written as

$$[\mathbf{G}] = [\mathbf{L}_G]^T[\mathbf{L}_G], \qquad (38)$$

in which $[\mathbf{L}_G]$ is an $n \times n$ real upper triangular random matrix such that

- random variables $\left\{[\mathbf{L}_G]_{jj'},\ j \le j'\right\}$ are independent;
- for $j < j'$, real-valued random variable $[\mathbf{L}_G]_{jj'}$ can be written as

$$[\mathbf{L}_G]_{jj'} = \delta(n+1)^{-1/2}U_{jj'}, \qquad (39)$$

in which $U_{jj'}$ is a real-valued Gaussian random variable with zero mean value and variance equal to 1;

- for $j = j'$, positive-valued random variable $[\mathbf{L}_G]_{jj}$ can be written as

$$[\mathbf{L}_G]_{jj} = \delta(n+1)^{-1/2}\sqrt{2V_j}, \qquad (40)$$

in which V_j is a positive-valued gamma random variable whose probability density function $p_{V_j}(v)$ with respect to dv

is written as

$$p_{V_j}(v) = \mathbb{1}_{\mathbb{R}^+}(v)\frac{1}{\Gamma(\alpha_{n,j})}v^{(\alpha_{n,j})^{-1}}e^{-v}, \quad \alpha_{n,j} = \frac{n+1}{2\delta^2} + \frac{1-j}{2}. \tag{41}$$

It should be noted that all the entries $\{[\mathbf{G}]_{jk}\}_{jk}$ are statistically dependent random variables.

5 NUMERICAL ILLUSTRATION FOR AN INDUSTRIAL BLADED DISK

The bladed disk considered is the same blisk used to validate the reduced-order model. This blisk is considered under rotation. Mistuning is modeled using the nonparametric probabilistic method and detuning is introduced by performing a shape modification of some blades and distributing them so that they create alternate detuning. For the forced response considerations, a conventional 9 engine order excitation is considered in the analysis over the excitation frequency range $\mathcal{B} = [4400, 4750]$ Hz. Forced response magnitude of the mistuned system is normalized with respect to the maximum magnitude of the equivalent tuned blisk under the same excitation conditions. The structural damping loss factor is set to 0.3%. For the reduced order model, the projection basis is constituted of modes belonging to the frequency band $[0, 5000]$ Hz.

5.1 Detuning method

Different types of intentional mistuning patterns have been adopted in the past, such as "alternate" mistuning, by alternating high- and low-frequency blades [22], periodic mistuning [23, 24], harmonic mistuning [6–8, 25], and linear mistuning [26]. The purpose here is not to find the best intentional mistuning pattern but to analyze the forced response sensitivity to mistuning, of a detuned system with a fixed chosen pattern. For the sake of simplicity, we only consider two types of blades : a reference blade (R) and a lower frequency blade (L). So the fixed pattern chosen here is 6R6L6R5L. To get the lower frequency blades, the blade shape is modified by removing locally 20% of the blade thickness on the upper part of the blade and adding locally 20% of the blade thickness on the lower part. This can be called a 20% modification. We present on Fig. 4, a 80% modification to highlight the geometric modification performed. To estimate the level of perturbation induced by this modification on aerodynamic characteristics, the Mach field (see Fig. 5) has been displayed on the different types of blades in cyclic symmetry configuration. Thus, we can see that the air flow has not greatly been perturbed, but little differences may appear on the damping characteristics of the two types of blade. These differences can be taken into account by the stochastic model of uncertainties, but to do so, we need a method for estimating the aeroelastic dispersion parameter between the two configurations like the one developed in [27]. For the sake of simplicity, this will not be treated here, and an aeroelastic null dispersion parameter is considered for the test.

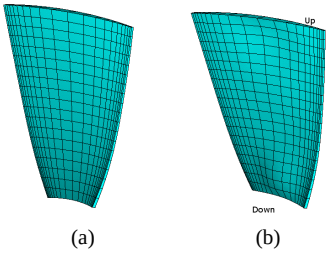

(a) (b)

Fig. 4. Reference blade shape (a) and modified blade shape (b).

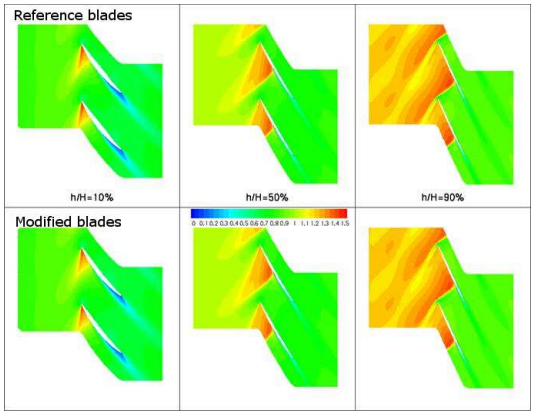

Fig. 5. Comparison of the Mach field on reference and modified blades.

5.2 Random magnification factor

Mistuning is expressed in terms of dispersion level on the stiffness matrix. In fact, in [27], by solving the inverse problem of specifying the blade manufacturing tolerances, it was found that the dispersion level of the mass matrix, induced by manufacturing tolerances, is about 1000 times less than the stiffness matrix one. The observation considered to control the forced responses is the random dynamic magnification factor $\{B(\omega), \omega \in \mathcal{B}\}$ which is such that

$$B(\omega) = \sup_{p\in\{0,\ldots,N-1\}} B^p(\omega), \qquad B^p(\omega) = \frac{|u^p(\omega)|}{\underline{u}^p_\infty},$$
$$\underline{u}^p_\infty = \sup_{\omega\in\mathcal{B}} |\underline{u}^p(\omega)|, \qquad B_\infty = \sup_{\omega\in\mathcal{B}} B(\omega), \tag{42}$$

in which for blade p, $u^p(\omega)$ is the random physical displacement of a tip node of the vibrating blade p, $\underline{u}^p(\omega)$ is the mean value of $u^p(\omega)$. The quantity B_∞ is the random dynamic magnification factor over the frequency band $\mathcal{B}$. The realizations of the random variable B_∞ are computed with the Monte Carlo numerical simulation and mathematical statistics are used for estimating the probability distribution. A convergence analysis has been carried out for the magnification factor. Since the second-order mean convergence yields the convergence in probability distribution, the convergence analysis has been limited to the second-order convergence of random magnification factor and damping coefficient. A 1000 Monte Carlo simulation has been performed for each

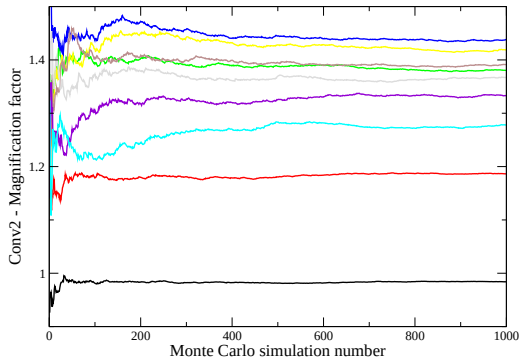

Fig. 6. Second-order mean convergence of B_∞ with mistuning: the curves, from the lower to the upper, correspond to a Monte Carlo simulation with 1000 realizations and for $\delta_K = 0.005, 0.01, 0.1, 0.02, 0.07, 0.06, 0.05, 0.04$ and 0.03.

value of δ_K and Fig. 6 shows that convergence is already reached for 500 simulations. Fig. 7 shows a well known be-

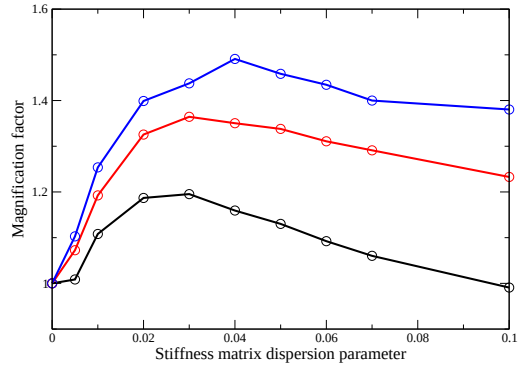

Fig. 7. Influence of the mistuning rate: graph such that $P(B_\infty \leq B_p) = p$. The lower, middle and upper curves correspond to a probability level of $p = 0.50, 0.95$ and 0.99.

havior of small mistuned bladed disks: the forced response increases for low rates of mistuning, reaches a maximum value and decreases slightly while the level of mistuning still increases.

5.3 Sensitivity analysis of mistuning for a given detuning

The purpose is to reduce the bladed disk sensitivity to mistuning by reducing the forced response magnification induced. Thus, we are interested in relatively small mistuning. A Monte Carlo simulation has also been performed with 1000 realizations for each value of δ_K and Fig. 8 shows that convergence is reached for 1000 realizations, although the bladed disk is detuned. The detuning performed is very effective for low mistuning levels as shown in Fig. 9. While the reference magnification factor has a well behavior, the detuned system magnification factor is lightly increasing but still remain under reference curve for the three probability

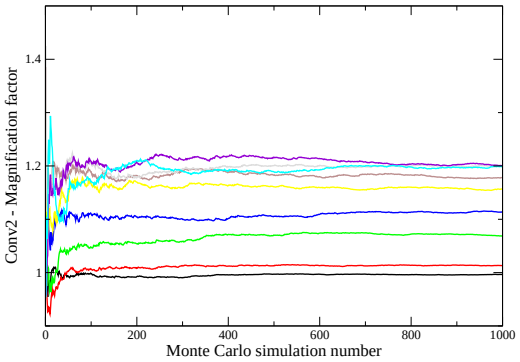

Fig. 8. Second-order mean convergence of B_∞ with mistuning and detuning: the curves, from the lower to the upper, correspond to a Monte Carlo simulation with 600 realizations and for $\delta_K = 0.005, 0.01, 0.01, 0.02, 0.04, 0.05, 0.1, 0.06$ and 0.07.

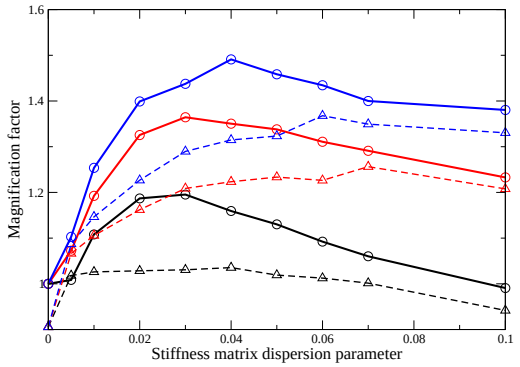

Fig. 9. Influence of the mistuning rate: graph such that $P(B_\infty \leq B_p) = p$. The solid curves with circles (and the dashed curves with triangles) are related to the tuned (and to the detuned) system. The lower, middle and upper curves correspond respectively to a probability level $p = 0.50, 0.95$ and 0.99.

levels which are considered. Moreover, at high mistuning levels, the detuned magnification factor curves tends to the reference one, showing that at high mistuning levels, the disorder degree is so high that the detuning performed is cover by the mistuning.

6 CONCLUSION

A methodology has been developed to perform the robust design of bladed disks in forced response with a detuning technic in presence of mistuning. Detuning is performed by modifying blade shapes without significantly perturbing the aeroelastic forces. Mistuning is taken into account by using a new reduction method (recently published) and the nonparametric probabilistic approach of both the system-parameter uncertainties and modeling errors. An example of reducing a bladed disk sensitivity to mistuning is presented. This analysis shows that although the detuning pattern is not optimized, the geometrical modifications of blades can reduce blade sensitivity to mistuning. Then, by combining blade geometric modifications with a detuning pattern op-

timization, as the one proposed in [5, 28], an optimal robust design model minimizing the forced responses, while keeping stability, can be obtained. This is the purpose of works in progress.

Acknowledgments
Turbomeca Company is gratefully acknowledged for the permission to publish this work.

References

[1] Whitehead, D., 1966. "Effects of Mistuning on the Vibration of Turbomachine Blades Induced by Wakes". *Journal of Mechanical Engineering Science,* **8**(1), pp. 15–21.

[2] Dye, R., and Henry, T., 1969. "Vibration Amplitudes of Compressor Blades Resulting from Scatter in Blade Natural Frequencies". *ASME Journal of Engineering for Power,* **91**(3), pp. 182–187.

[3] Capiez-Lernout, E., and Soize, C., 2004. "Nonparametric Modeling of Random Uncertainties for Dynamic Response of Mistuned Bladed-disks". *ASME Journal of Engineering for Gas Turbines and Power,* **126**(3), pp. 610–618.

[4] Ewins, D., 1969. "The Effects of Detuning upon the Forced Vibrations ofBladed Disks". *Journal of Sound and Vibration,* **9**(1), pp. 65–69.

[5] Choi, B.-K., Lentz, J., Rivas-Guerra, A., and Mignolet, M., 2003. "Optimization of Intentional Mistuning Patterns for the Reduction of the Forced Response Effects of Unintentional Mistuning: Formulation and Assessment". *ASME Journal of Engineering for Gas Turbines and Power,* **125**, pp. 131–140.

[6] Castanier, M., Ottarson, G., , and Pierre, C., 1997. "Reduced Order Modeling Technique for Mistuned Bladed Disks". *ASME Journal of Vibration and Acoustics,* **119**(3), pp. 439–447.

[7] Castanier, M., and Pierre, C., 2002. "Using Intentional Mistuning in the Design of Turbomachinery rotors". *AIAA Journal,* **40**(10), pp. 2077–2086.

[8] Mignolet, M., Hu, W., and Jadic, I., 2000. "On the Forced Response of Harmonically and Partially Mistuned Bladed Disks. part 1: Harmonic Mistuning, part 2: Partial Mistuning and Applications". *International Journal of Rotating Machinery,* **6**(1), pp. 29–56.

[9] Bladh, R., Castanier, M., and Pierre, C., 1999. "Reduced order modeling and vibration analysis of mistuned bladed disk assemblies with shrouds". *ASME Journal of Engineering for Gas Turbines and Power,* **121**(3), pp. 515–522.

[10] Bladh, R., Castanier, M., and Pierre, C., 2001. "Component-mode-based reduced order modeling techniques for mistuned bladed disks - part i: Theoretical models". *ASME Journal of Engineering for Gas Turbines and Power,* **123**(1), pp. 89–99.

[11] Yang, M.-T., and Griffin, J., 2001. "A Reduced-Order Model of Mistuning using a Subset of Nominal System Modes". *ASME Journal of Engineering for Gas Turbines and Power,* **123**(3), pp. 893–900.

[12] Feiner, D., and Griffin, J., 2002. "A fundamental model of mistuning for a single family of modes". *Journal of Turbomachinery,* **124**, pp. 597–605.

[13] Feiner, D., and Griffin, J., 2002. "Mistuning identification of bladed disks using fundamental mistuning model. part 1: Theory, part 2: Application". *Journal of Turbomachinery,* **126**, pp. 150–165.

[14] Lim, S.-H., Castanier, M., and Pierre, C., 2004. "Vibration modeling of bladed disks subject to geometric mistuning and design changes". In Proceedings of the 45-th AIAA/ASME/ASCE/AHS/ASC Structures, Structural Dynamics and Material Comference, paper 2004-1686, Palm Springs, California, USA.

[15] Martel, C., Corral, R., and Llorens, J., 2008. "Stability increase of aerodynamically unstable rotor using intentional mistuning". In Proceedings of the ASME TURBO EXPO 2008.

[16] Martel, C., and Corral, R., 2008. "Asymptotic description of maximum mistuning amplification of bladed disk forced response". In Proceedings of the ASME TURBO EXPO 2008.

[17] Sinha, A., 2009. "Reduced-order model of a bladed rotor with geometric mistuning". *Journal of Turbomachinery - Transaction of the ASME,* **131**, pp. 031007.1 – 031007.7.

[18] Ganine, V., Legrand, M., Pierre, C., and Michalska, H., 2008. "A reduction technique for mistuned bladed disks with superposition of large geometric mistuning and small model uncertainties". In Proceedings of the 12-th International Symposium on Transport Phenomena and Dynamics of Rotating Machinery, paper 2008–20158, Honolulu, Hawaii, USA.

[19] Mbaye, M., Soize, C., and Ousty, J.-P., 2010. "A reduced-order model of detuned cyclic dynamical systems with geometric modifications using a basis of cyclic modes". *ASME Journal of Engineering for Gas Turbines and Power,* **132**(11), pp. 112502–1–9.

[20] Soize, C., 2001. "Maximum Entropy Approach for Modeling Random Uncertainties in Transient Elastodynamics". *Journal of the Acoustical Society of America,* **109**(5), pp. 1979–1996.

[21] Soize, C., 2005. "Random Matrix Theory for Modeling Uncertainties in Computational Mechanics". *Computer Methods in Applied Mechanics and Engineering,* **194**, pp. 1333–1366.

[22] Griffin, J. H., and Hoosac, T. M., 1984. "Model development and statistical investigation of turbine blade mistuning". *ASME Journal of Vibration, Acoustics, Stress, and Reliability in Design,* **106**, pp. 204–210.

[23] Imregun, M., and Ewins, D. J., 1984. "Aeroelastic vibration analysis of tuned and mistuned bladed systems". In Proceedings of the Second Symposium on Unsteady Aerodynamics of Turbomachines and Propellers, Cambridge, UK.

[24] Rzadkowski, R., 1993. "The general model of free vibrations of mistuned bladed discs, part 1: Theory, part

2: Numerical results". *Journal of Sound and Vibration*, **173**(3), pp. 377–393.

[25] Kenyon, J. A., and Griffin, J. H., 2001. "Forced response of turbine engine bladed disks and sensitivity to harmonic mistuning". In Proceedings of the ASME TURBO EXPO 2001, 2001-GT-0274.

[26] Jones, W. J., and Cross, C. J., 2002. "Reducing mistuned bladed disk forced response below tuned resonant amplitudes". In Seventh National Turbine Engine High Cycle Fatigue Conference, Palm Beach, FL, USA.

[27] Capiez-Lernout, E., Soize, C., Lombard, J.-P., Dupont, C., and Seinturier, E., 2005. "Blade Manufacturing Tolerances Definition for a Mistuned Industrial Bladed Disk". *ASME Journal of Engineering for Gas Turbines and Power*, **127**(2), pp. 621–628.

[28] Han, Y., and Mignolet, M., 2001. "Optimization of intentional mistuning patterns for the mitigation of the effects of random mistuning". In Proceedings of the ASME TURBO EXPO 2008, GT-2008-51439.